TA4 - 9:00

JOINT-BASED CONTROL OF A NONLINEAR MODEL OF A FLEXIBLE ARM

Alessandro De Luca

Dipartimento di Informatica e Sistemistica
Università di Roma "La Sapienza"
Via Eudossiana 18, 00184 Roma, Italy

Bruno Siciliano

Dipartimento di Informatica e Sistemistica
Università di Napoli
Via Claudio 21, 80125 Napoli, Italy

Abstract. In this paper the control problem for a one-link flexible arm described by a nonlinear model is considered. Based on the input-output inversion algorithm, a state-feedback control law is designed which enables exact reproduction of any desired smooth joint trajectory. In the closed loop an unobservable dynamics naturally arises, related to the variables describing the arm distributed flexibility. Open vs. closed-loop strategies are developed and compared. Simulation results are included. Finally, extensions of this approach to end-point based trajectory control are suggested.

1. Introduction

Lightweight flexible structures have been recognized as offering a potential over current rigid and massive designs [1]. Increasing attention has been paid lately to the control problem of flexible robotic arms. Accurate dynamic modeling is a requisite for improved performance. Most of the existing approaches are based on classical control methods since linear models are used [2-5]. Other works utilize nonlinear models and different control techniques, such as adaptive control [6], singular perturbation [7], and pseudo-linearization [8].

A proper definition of what are the control objectives to be pursued for flexible arms has not been established yet. One might be interested in regulating the end-point around a final position, or in tracking joint trajectories while limiting arm deflections, or even in driving the end-point along a feasible path. This paper addresses the following questions: i) is it possible to exactly reproduce any given joint trajectory?, and ii) is the resulting closed-loop system stable? It will be shown that the answer is yes to both questions.

In particular, a nonlinear control law that meets these requirements can be designed using the input-output inversion algorithm [9]. It is worth mentioning here that the inversion approach has been used already in rigid arm control [10] and is equivalent to the well-known computed torque method [11]. The same approach has been successfully applied in the case of robot arms with elasticity concentrated at the joints [12].

The most relevant result of using inversion-based feedback control in the above two robotic applications is the equivalence of the obtained closed-loop system to a linear and decoupled one, i.e. to strings of input-output integrators. However, when the same technique is applied to flexible arms the *full linearization property* is lost. In the closed loop, a subsystem arises whose dynamics is unobservable from the output and possibly nonlinear. The internal stability of this subsystem has to be verified in order to validate the chosen control design. This issue is completely absent in the case of rigid arms or when elasticity is concentrated at the same locations of the control inputs. As a matter of fact, when the output is chosen to be the joint angle of the flexible arm, the unobservable dynamics is the one associated with the elastic variables which describe the arm deformation. Although this dynamics is shown to be stable, still a critical point is how damped is this part.

The implementation of control laws based on system inversion presents other interesting aspects. A closed-loop strategy requires nonlinear static feedback from the *full* state of the arm. On the other hand, pre-computation of open-loop torques capable of driving the joint angle along a given time trajectory asks for the *off-line integration* of a reduced order dynamic system. This is needed for recovering the "desired" behavior of the deflection associated to the assigned joint trajectory. The stability properties of this reduced order dynamics are closely related to the ones of the unobservable dynamics arising in the closed-loop strategy [13].

The paper is organized as follows. Section 2 contains the dynamic model of a one-link flexible arm using any number of assumed modes. In Section 3, open and closed-loop joint-based control laws are derived. Also, their stability is briefly analyzed. The results of a simulation study which compares these strategies and tests for robustness are described in Section 4. A discussion of the possible extensions for controlling directly the motion of the tip point or of any other point on the structure completes the paper.

2. Dynamic model

The one-link flexible arm of Figure 1 is considered. The arm moves on a horizontal plane and is stiff w.r.t. torsional effects. A solution to the flexible motion of the link can be obtained through modal analysis, under the assumption of small deflections

$$y(\eta,t) = \sum_{i=1}^{m} \delta_i(t)\, \phi_i(\eta)$$

ϕ_i is the eigenfunction expressing the displacement of the i-th assumed mode of link deflection, δ_i is the time-varying amplitude of the i-th mode, and m is the number of modes

used to describe the distributed link deformation.

For a clamped-free vibrating beam the orthonormal modal eigenfunctions are given by

$$\phi_i(\xi) = \sin(\beta_i\xi) - \sinh(\beta_i\xi) + \nu_i(\cos(\beta_i\xi) - \cosh(\beta_i\xi))$$

$$\nu_i = \frac{\sin\beta_i + \sinh\beta_i}{\cos\beta_i + \cosh\beta_i} \qquad \beta_i^4 = \frac{\rho A(2\pi\omega_i)^2 L^4}{EI}$$

for i = 1,...,m, where $\xi = \eta / L$ is the normalized position along the beam of length L, A is the beam cross area, E is its Young's modulus, I is the beam area inertia, ρ its density, and ω_i is the frequency of the i-th mode.

The dynamic equations for the one-link flexible arm are derived following a Lagrangian approach [7] and can be written in the form

$$B(\delta)\begin{bmatrix}\ddot{\theta}\\ \ddot{\delta}\end{bmatrix} + \begin{bmatrix}n_1(\dot{\theta},\delta,\dot{\delta})\\ n_2(\dot{\theta},\delta)\end{bmatrix} + \begin{bmatrix}0\\ K\delta + F\dot{\delta}\end{bmatrix} = \begin{bmatrix}u\\ 0\end{bmatrix}$$

where θ is the joint variable, $\delta = (\delta_1 \dots \delta_m)^T$ is the vector of deflections, u is the control torque at the joint location.

The elements b_{ij} of the positive definite symmetric inertia matrix $B(\delta)$ takes on the expressions

$$b_{11}(\delta) = J_0 + M_L L^2 + I_0 + M_L(\Phi_e^T\delta)^2$$

$$b_{1j} = M_L\,\phi_{j-1,e} + w_{j-1}, \qquad j = 2,\dots,m+1$$

$$b_{ii} = m_b + M_L\,\phi_{i-1,e}^2 + J_L\,\phi'^2_{i-1,e}, \qquad i = 2,\dots,m+1$$

$$b_{ij} = M_L\,\phi_{i-1,e}\phi_{j-1,e} + J_L\,\phi'_{i-1,e}\phi'_{j-1,e}, \qquad i = 2,\dots,m+1,\ j \neq i$$

with

$$\Phi_e^T = \begin{bmatrix}\phi_{1e} & \cdots & \phi_{me}\end{bmatrix} \qquad \phi_{ie} = \phi_i(\xi)\Big|_{\xi=1}$$

$$\Phi'^T_e = \begin{bmatrix}\phi'_{1e} & \cdots & \phi'_{me}\end{bmatrix} \qquad \phi'_{ie} = \frac{d\phi_i(\xi)}{d\xi}\Big|_{\xi=1}$$

$$w_i = \rho A L^2 \int_0^1 \phi_i(\xi)\,\xi\,d\xi \qquad i = 1,\dots,m$$

where m_b and M_L are respectively the beam and the load mass, I_0 and J_L are the joint and the load inertia, and J_0 is the beam inertia relative to the joint.

The nonlinear terms n_1 and n_2 can be computed by differentiation of the elements of the inertia matrix and represents Coriolis and centrifugal terms

$$n_1(\dot{\theta},\delta,\dot{\delta}) = 2M_L\dot{\theta}\,(\Phi_e^T\delta)^T(\Phi_e^T\dot{\delta})$$

$$n_2(\dot{\theta},\delta) = -M_L\dot{\theta}^2\,(\Phi_e\Phi_e^T)\,\delta$$

K is an equivalent spring constant matrix

$$K = \mathrm{diag}\{k_1, \dots, k_m\}$$

$$k_i = \frac{EI}{L^3}\int_0^1 \left[\frac{d^2\phi_i(\xi)}{d\xi^2}\right]^2 d\xi$$

F is a diagonal damping matrix accounting for the internal viscous friction in the flexible structure. Enhancement of such a *passive* damping is a feasible alternative to active modal control [14].

Since the clamped-free assumption has been made for the vibrating beam, there is no displacement at the joint location. As a consequence, no control input appears in the left hand side of the lower m dynamic equations. Note also that the arm model is independent from the joint angle value θ, due to the symmetry of system dynamics around the joint axis.

In the following, the inverse $D(\delta)$ of the system inertia matrix will be used. $B(\delta)$ can be conveniently partitioned into four blocks

$$B(\delta) = \begin{bmatrix}b_{11}(\delta) & B_{12}^T\\ B_{12} & B_{22}\end{bmatrix}$$

with B_{22} of order mxm. Accordingly, the inverse can be written explicitly as

$$D(\delta) = B^{-1}(\delta) = \begin{bmatrix}d_{11}(\delta) & D_{12}^T(\delta)\\ D_{12}(\delta) & D_{22}(\delta)\end{bmatrix}$$

with

$$d_{11}(\delta) = \frac{1}{b_{11}(\delta) - B_{12}^T B_{22}^{-1} B_{12}}$$

$$D_{12}(\delta) = -\frac{\Delta^{-1}(\delta)\,B_{12}}{b_{11}(\delta)} \qquad D_{22}(\delta) = \Delta^{-1}(\delta)$$

and

$$\Delta(\delta) = B_{22} - \frac{B_{12}\,B_{12}^T}{b_{11}(\delta)}.$$

3. Joint-based inversion control

The definition of outputs for a given dynamical system is closely related to the chosen control objective. When a scalar output y is associated to the flexible arm system, one can derive the input torque u which is capable of reproducing exactly a given trajectory $y_d(t)$ as output, based on system inversion techniques.

In particular, if a joint-based strategy is pursued

$$y = \theta$$

Applying the inversion algorithm [9], it is easy to see that the input u appears explicitly in the second derivative of the output function

$$\ddot{y} = d_{11}(\delta)\,[u - n_1(\dot{\theta},\delta,\dot{\delta})] - D_{12}^T(\delta)\,[n_2(\dot{\theta},\delta) + K\delta + F\dot{\delta}]$$

Since $d_{11}(\delta) \neq 0$ always, this is true no matter what flexible arm is considered or how many modes are assumed.

Let a = a(t) be the desired output acceleration. The relative control torque is obtained then setting

$$\ddot{y} = a$$

in the above equation and solving for u as

$$u = n_1(\dot{\theta},\delta,\dot{\delta}) + \frac{1}{d_{11}(\delta)}\,[a + D_{12}^T(\delta)\,(n_2(\dot{\theta},\delta,\dot{\delta}) + K\delta + F\dot{\delta})]$$

$$= u^*(a,\dot{\theta},\delta,\dot{\delta})$$

The input torque u* yields the tracking of the desired output trajectory. Indeed, exact reproduction is guaranteed only if the trajectory is of class C^1 (i.e. with at most step discontinuities in acceleration) and if there is matching with the initial conditions, in this case with joint position and velocity. Otherwise, only asymptotic tracking results.

The above control law can be implemented in an open or in a closed-loop scheme. Assume that a desired smooth joint trajectory $\theta = \theta_d(t)$ has been given, together with its time derivatives.

3.1 Open-loop control

In this scheme set

$$\dot{\theta} = \dot{\theta}_d(t) \qquad a = \ddot{\theta}_d(t)$$

The control u* is not completely specified by the above identities since the knowledge of $\delta(t)$ and $\delta'(t)$ is still needed. This is essentially different from the case of rigid arms where assigning the behavior to the joint variables uniquely determines the required torque inputs. Here, a dynamic generator has to be set up to recover the time evolution of the elastic coordinates δ associated to the desired joint trajectory. This generator is obtained by plugging the expression of u* into the dynamic equations, replacing then the joint variables by their desired values. As a result

$$\ddot{\delta} = - B_{22}^{-1} [B_{12}^T \ddot{\theta}_d + n_2(\dot{\theta}_d , \delta) + K\delta + F\dot{\delta}]$$

The off-line integration of these m second-order differential equations, starting from $(\delta(0), \delta'(0))$, yields the time evolutions $(\delta_d(t), \delta'_d(t))$. If the above dynamics were unstable, the whole process of generation of the open-loop torque would be unfeasible. Note that these differential equations are *linear* time-varying ones and can be rewritten in state-space format as

$$\begin{bmatrix} \delta \\ \dot{\delta} \end{bmatrix} = \begin{bmatrix} 0 & I \\ A_{21}(\theta_d) & A_{22} \end{bmatrix} \begin{bmatrix} \delta \\ \dot{\delta} \end{bmatrix} + \begin{bmatrix} 0 \\ b_2(\theta_d) \end{bmatrix} = A(t) \begin{bmatrix} \delta \\ \dot{\delta} \end{bmatrix} + b(t)$$

with

$$A_{21}(\theta_d) = - B_{22}^{-1} [K - M_L \ddot{\theta}_d (\Phi_e \Phi_e^T)]$$

$$A_{22} = - B_{22}^{-1} F \qquad b_2(\ddot{\theta}_d) = - B_{22}^{-1} B_{12} \ddot{\theta}_d$$

The resulting open-loop torque to be applied at the joint is then

$$u_{OL} = u^*(\ddot{\theta}_d, \dot{\theta}_d, \delta_d, \dot{\delta}_d)$$

To gain some robustness at low expense, a linear feedback can be used in addition to this reference torque signal. A PD controller on the joint trajectory error is properly designed as

$$u_{OL,PD} = u^*(\ddot{\theta}_d, \dot{\theta}_d, \delta_d, \dot{\delta}_d) + \frac{1}{d_{11}(\delta_d)} [k_p(\theta_d - \theta) + k_v(\dot{\theta}_d - \dot{\theta})]$$

Note that this kind of law does not require any measurement of arm deflection.

3.2 Closed-loop control

In this case u* is computed by feeding back the full state $(\theta, \theta', \delta, \delta')$ of the flexible arm. The resulting closed-loop system equations are given by

$$\ddot{\theta} = a \qquad y = \theta$$

$$\ddot{\delta} = - B_{22}^{-1} [B_{12}^T a + n_2(\dot{\theta}, \delta) + K\delta + F\dot{\delta}]$$

The input-output behavior from the external input a to y has been linearized by the inversion control law u*. Thus, a linear PD law on the joint trajectory error is used for stabilizing the input-output double integration path. By choosing a as

$$a = \ddot{\theta}_d + k_v(\dot{\theta}_d - \dot{\theta}) + k_p(\theta_d - \theta)$$

with $k_p > 0$ and $k_v > 0$, one obtains

$$u_{CL,PD} = u^*(\ddot{\theta}_d, \dot{\theta}, \delta, \dot{\delta}) + \frac{1}{d_{11}(\delta)} [k_p(\theta_d - \theta) + k_v(\dot{\theta}_d - \dot{\theta})]$$

Once this feedback control has been applied, an unobservable part related to the dynamics of the elastic variables δ arises (see also Figure 2). The closed-loop stability of this sink plays a crucial role in the whole proposed control design. In particular, one is interested in the behavior of the elastic variables when the trajectory is completed. This describes the way arm vibrations damp out near the final trajectory point, and thus accounts for the positional accuracy of the arm tip.

The study of the dynamics of the unobservable part in these conditions is closely related to the so-called zero-dynamics of the given nonlinear system [15]. Setting $y(t) = 0$ for all times implies $y' = \theta' = 0$ and $y'' = a = 0$. Replacing these values into the closed-loop dynamics of δ gives

$$\ddot{\delta} = - B_{22}^{-1} [n_2(0,\delta) + K\delta + F\dot{\delta}] = - B_{22}^{-1} [K\delta + F\dot{\delta}]$$

using the fact that n_2 is quadratic in the joint velocity. Thus, the internal arm dynamics associated with a constant zero value of the joint output becomes a *linear* one. When $F = 0$, since K and B_{22} are positive definite matrices, the 2m eigenvalues are all complex pairs located on the imaginary axis and the system is critically stable. As soon as some passive damping is present, i.e. $F > 0$, these closed-loop roots move to the open left half-plane and asymptotic internal stability is obtained.

The above analysis holds only at the terminal point of the trajectory. Indeed, one has also to guarantee that the elastic deflections are kept limited during the point-to-point motion in order to avoid too much stressing of the beam. The simulations reported in the next section confirm that this is indeed the case. Note that the deflected configuration of the arm at the end of the trajectory provides the initial conditions for the above linear differential equations governing the residual oscillatory behavior.

In general, it is quite difficult to extract accurate information about the structural damping. Thus, it seems reasonable to take out the term $F\delta'$ from the control law u*. The resulting closed-loop system will be described by

$$\ddot{\theta} = a - D_{12}^{T}(\delta)\, F\, \dot{\delta}$$

$$\ddot{\delta} = -B_{22}^{-1}[\, B_{12}^{T} a + n_2(\dot{\theta}, \delta) + K\delta\,] - D_{22}(\delta)\, F\dot{\delta}$$

It follows that exact tracking of joint trajectories is not possible anymore. The actual trajectory will typically lag behind the desired one by a small amount depending on the modal damping coefficients in F. However, the stability properties are preserved.

4. Simulation results

The above joint-based inversion control laws have been simulated using the two-modes model of the one-link flexible arm considered in [3,7]. The first two eigenfrequencies of this 4 ft long arm are 2.12 and 14.3 Hz. The equivalent spring coefficients associated to the two considered modes are $k_1 = 5.54$ and $k_2 = 198.56$.

The desired trajectory specifies a joint motion from $\theta(0) = 0$ to $\theta(T) = 90$ deg, with a velocity profile $\theta_d'(t) = (90/T)\,[1 - \cos(360\, t/T)]$ deg/sec, where $T = 2$ sec. The gains of the linear PD controllers used for the input-output stabilization are the same for all simulations, and are chosen as $k_p = 2500$, $k_v = 100$, corresponding to a critical response with a double pole at -50.

Figures 3-5 show the results of a 4 sec simulation, when the closed-loop scheme with $u_{CL,PD}$ is used for the arm without passive damping ($F = 0$). The sampling time is 1 msec. The plots are respectively the joint error, the x-component of the end-effector error, and the torque input. The time-behavior of the two flexible modes is reported in Figures 6-7. The desired joint trajectory is reproduced accurately (.006 deg as maximum error) and even less error could be obtained with higher gains. However, the oscillations left in the arm result in small displacements of the tip around the final point. These are of the order of .01 ft. Note that some control effort is present also after $T = 2$ sec, and is needed for keeping the joint angle at its desired final value.

Figures 8-9 are relative to a doubling in value of the load parameters M_L and J_L. Ripples are present in the joint position error, but the achieved result indicates the robustness of the control scheme w.r.t. these variations.

In Figures 10-11 the open-loop strategy $u_{OL,PD}$ is evaluated for the nominal plant. Although in this case the joint maximum error is doubled and the joint angle keeps on oscillating even after $T = 2$ sec, the end-effector error is practically the same as in closed-loop control. Also the required torque input, not reported here, is very similar. Thus, a cheap implementation of the proposed inversion control law, with no use of deformation measures, is a feasible alternative.

The effects of a passive damping in the structure is investigated next. A diagonal matrix F is added to the model, with elements $f_i = 0.2\ (k_i)^{1/2}$, $i = 1,2$. In the control law no compensation of this damping is done. The benefits of this structural modification are apparent from Figures 12-13, which refer to closed-loop control with a doubling of load parameters. A small delay in the tracking of the joint trajectory can be recognized. On the other hand, oscillations in the tip position vanish immediately after the completion of the joint trajectory.

Not surprisingly, passive damping is of great help also in the case of open-loop control as shown in Figures 14-15 for the nominal case.

5. Discussion

It has been shown that any assigned smooth joint trajectory can be exactly reproduced for matched initial conditions using inversion control techniques. Closed-loop and open-loop strategies were compared. If a good dynamic model is available, open-loop computation of joint torque plus a linear PD joint trajectory controller yields a satisfactory performance, particularly when passive damping is present in the flexible arm. The above results were obtained for a one-link robotic arm, but it is easy to see that the joint-based approach can be extended in general to multi-link flexible arms.

When dealing with robot arms, the most relevant concern should be the accurate control of the end-effector behavior. Indeed, joint-based strategies are only a means for obtaining this goal. Another issue to be better understood is the relevance of the problem of *exact tracking* of trajectories for the arm tip w.r.t. *regulation* around the trajectory final point. In any case, the oscillatory behavior of the flexible arm should be kept limited, and possibly under a prescribed level, even when exact joint trajectory following is achieved.

Extensions could be made to the proposed approach to cope with the above requirements. Some alternatives are discussed next.

a) Inversion control for end-point motion. This may seem the most natural modification of the joint-based strategy. Unfortunately, the design of a controller capable of reproducing exactly smooth trajectories for the arm tip leads in general to unstable behavior. This is due to the non-minimum phase nature of the end-effector control problem for flexible arms [2,5,13]. Some results on end-effector trajectory control were obtained in [4], using an approximate linear model of a one-link flexible arm. It is well-known that in the linear case, input-output inversion for *all* smooth trajectories is not possible if the plant has zeros in the right-plane.

A nonlinear equivalent can be given to the concept of non-minimum phase linear systems, i.e. a nonlinear system with unstable zero-dynamics [15]. For the model of the arm considered in the previous section, one can define as output

$$y = \theta + \frac{\phi_1\, \delta_1 + \phi_2\, \delta_2}{L}$$

which is the linearized expression of the angle pointing at the arm end-point. An inversion-based control law leads to a fourth-order nonlinear unobservable subsystem in the closed loop which is unstable. In fact, by just looking at the linear approximation around $\delta'_1 = \delta'_2 = 0$ of the zero-dynamics, one finds in this case two pairs of real poles in $s_{1,2} = \pm 12.95$ and $s_{3,4} = \pm 79.43$.

As a result, limited confidence should be given to *exact* reproduction of end-point trajectories. Probably, a slight relaxation of this constraint leads to a successfull design.

b) Addition of active damping control. In this case the joint-based strategy is modified by the parallel addition of a controller which tries to limit arm deflections and/or end-point errors. Of course, exact reproduction of trajectories in the joint space is lost.

A modal damping approach was proposed in [16], where LQ techniques have been used; the derivation is somewhat involved and the method works only in a local fashion, since it requires linearization around a point.

The design of two-time scales controllers in the singular perturbation approach [7] follows a similar phylosophy for reducing the vibrational behavior. As a matter of fact, the *fast* linear control ensures limited deflections around the motion prescribed by the slow control law. Note that, in principle, the latter may be replaced by the joint-based inversion control proposed here.

c) Inversion control for the motion of a point on the arm. A third hybrid method may be devised, based on the following considerations. There may exist one or more points along the structure, other than at the arm joint, for which an exact trajectory can be assigned without the occurrence of instabilities. If so, this point will safely behave in a "rigid" way. For a one-link flexible arm it is convenient to define as output the joint angle pointing to a generic point along the arm. A simple scalar parametrization of such an output follows. Thus, a critical value of this parameter separates the outputs (i.e. the points on the arm) which give rise to a stable behavior from those leading to unstable behavior of the closed-loop unobservable part. Indeed, the joint-based output considered in this paper belongs to the first class while the arm end-point is usually an element of the latter.

In linear models, beyond this critical output point the system has a transfer function with non-minimum phase zeros. Since in the nonlinear case this critical point moves along the structure during system operation, a conservative choice should be taken.

With this approach one is able to control exactly the motion of a certain point located on the arm, using inversion techniques. The underlying assumption is that the closer this point is to the end-effector, the smaller the tip oscillations will be - although possibly of higher frequency -

The feasibility of this design has been shown in [13] for a simple arm with concentrated flexibility and is now under investigation for more realistic models of flexible arms.

References

[1] Book, W.J., New concepts in lightweight arms, *2nd Int. Symp. Robotics Research*, Kyoto, 1984.

[2] Cannon Jr., R.H., Schmitz, E., Initial experiments on the end-point control of a flexible one-link robot, *Int. J. Robotics Research*, **3**, 3, 62-75, 1986.

[3] Hastings, G.G., Book, W.J., Experiments in optimal control of a flexible arm, *American Control Conf.*, Boston, 1985.

[4] Bayo, E., A finite-element approach to control the end-point motion of a single-link flexible robot, *J. of Robotic Systems*, **4**, 63-75, 1987.

[5] Canudas de Wit, C., Van den Bossche, E., Adaptive control of a flexible arm with explicit estimation of the payload mass and friction, *IFAC Symp. on Theory of Robots*, Vienna, 1986.

[6] Siciliano, B., Yuan, B.S., Book, W.J., Model reference adaptive control of a one link flexible arm, *25th IEEE Conf. on Decision and Control*, Athens, 1986.

[7] Siciliano, B., Book, W.J., A singular perturbation approach to control of lightweight flexible manipulators, to appear on *Int. J. Robotics Research*, 1988.

[8] Nicosia, S. Tomei, P., Tornambè, A., Nonlinear controller and observer for a single-link flexible manipulator, *4th IEEE Conf. on Robotics and Automation*, Raleigh, 1987.

[9] Hirschorn, R.M., Invertibility of multivariable nonlinear control systems, *IEEE Trans. Automatic Control*, **24**, 855-865, 1979.

[10] Singh, S.N., Schy, A.A., Invertibility and robust nonlinear control of robotic systems, *23rd IEEE Conf. on Decision and Control*, Las Vegas, 1984.

[11] Bejczy, A.K., Robot arm dynamics and control, Jet Propulsion Lab, California Institute of Technology, TM 33-669, 1974.

[12] De Luca, A., Dynamic control of robots with joint elasticity, *5th IEEE Conf. on Robotics and Automation*, Philadelphia, 1988.

[13] De Luca, A., Lucibello, P., Ulivi, G., Inversion techniques for open and closed-loop control of flexible robot arms, *2nd Int. Symp. on Robotics and Manufacturing Research*, Albuquerque, November 1988.

[14] Book, W.J., Dickerson, S.L., Hastings, G., Cetikunt, S., Alberts, T., Combined approaches to lightweight arm utilization, *ASME Winter Annual Meeting*, Miami, 1985.

[15] Isidori, A., Moog, C.H., On the nonlinear equivalent of the notion of transmission zeros, *Modeling and Adaptive Control*, (C.I.Byrnes, K.H.Kurszanski Eds.) Springer Verlag, 1987.

[16] Singh, S.N., Schy, A.A., Robust torque control of an elastic robotic arm based on invertibility and feedback stabilization, *24th IEEE Conf. on Decision and Control*, Ft.Lauderdale, 1985.

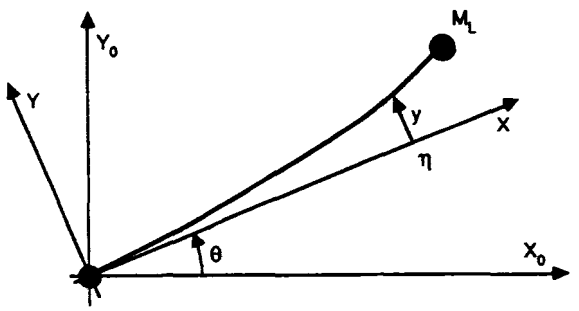

Figure 1 - The one-link flexible arm

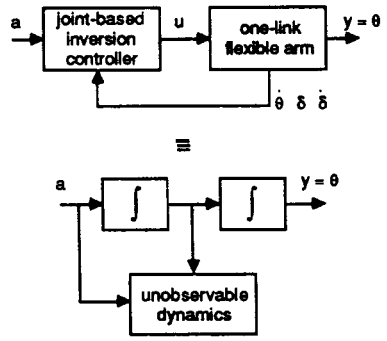

Figure 2 - Closed-loop inversion control

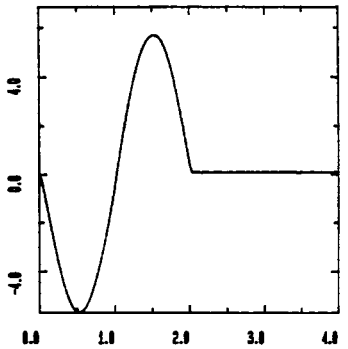

Figure 3 - Closed-loop control
Joint error [10 -3 deg]

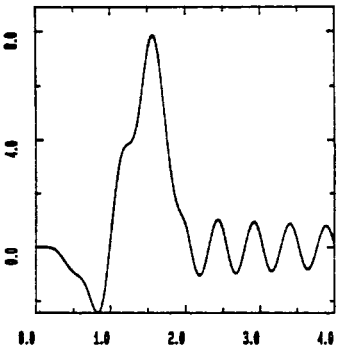

Figure 4 - Closed-loop control
End-point error [10 -2 ft]

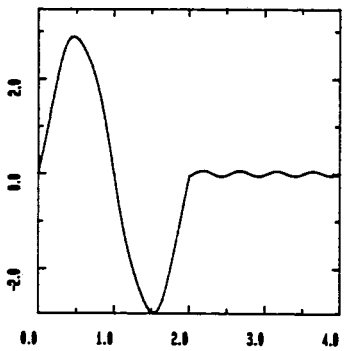

Figure 5 - Closed-loop control
Input torque [ft lb]

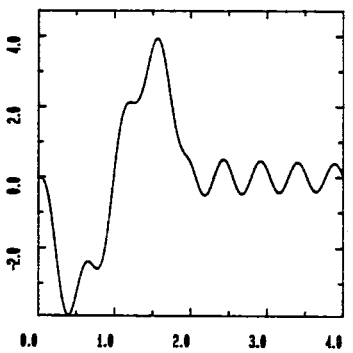

Figure 6 - Closed-loop control
First mode [10 -2 ft]

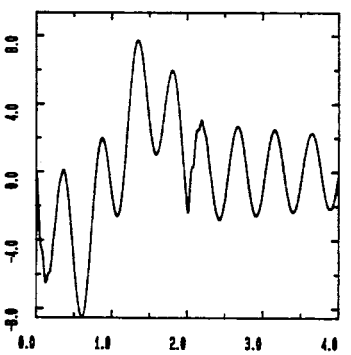

Figure 7 - Closed-loop control
Second mode [10 -5 ft]

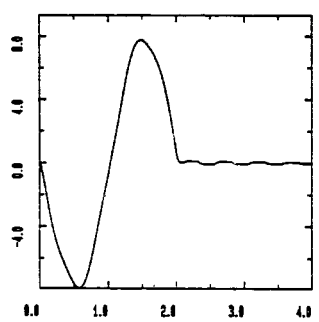

Figure 8 - Closed-loop control, double load
Joint error [10 -3 deg]

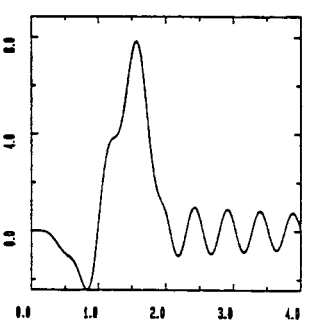

Figure 9 - Closed-loop control, double load
End-point error [10 -2 ft]

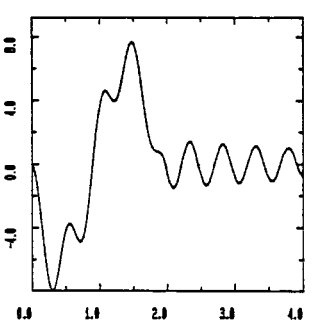

Figure 10 - Open-loop control
Joint error [10 -3 deg]

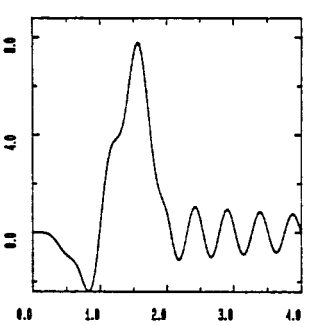

Figure 11 - Open-loop control
End-point error [10 -2 ft]

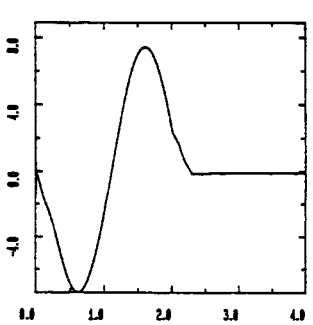

Figure 12 - Closed-loop control, double load, F > 0, Joint error [10 -3 deg]

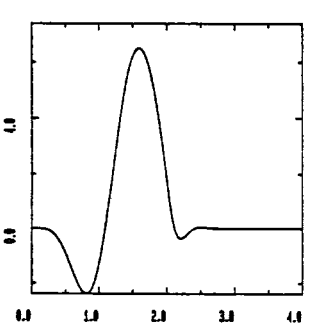

Figure 13 - Closed-loop control, double load, F > 0, End-point error [10 -2 ft]

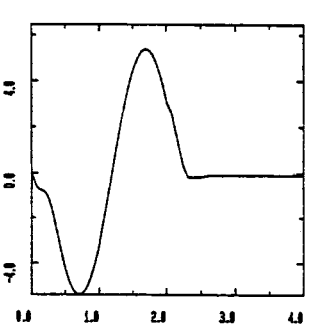

Figure 14 - Open-loop control, F > 0
Joint error [10 -3 deg]

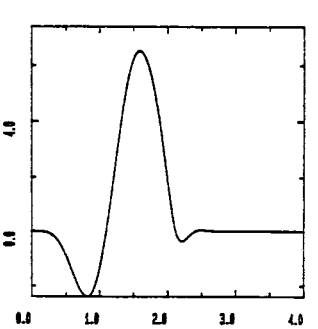

Figure 15 - Open-loop control, F > 0
End-point error [10 -2 ft]